THE JOURNAL OF BIOLOGICAL CHEMISTRY Vol. 273, No. 4, Issue of January 23, pp. 2044–2051, 1998
Printed in U.S.A.

Mechanism of Acidification of the *trans*-Golgi Network (TGN)

IN SITU MEASUREMENTS OF pH USING RETRIEVAL OF TGN38 AND FURIN FROM THE CELL SURFACE*

(Received for publication, August 19, 1997, and in revised form, November 13, 1997)

Nicolas Demaurex‡§, Wendy Furuya¶, Sudhir D'Souza¶‖, Juan S. Bonifacino, and Sergio Grinstein¶‡‡**

*From the ‡Department of Physiology, University Medical Center, Geneva, CH 1211, Switzerland, **Cell Biology and Metabolism Branch, NICHD, National Institutes of Health, Bethesda, Maryland 20892, and ¶Division of Cell Biology, Hospital for Sick Children, Toronto, M5G 1X8, Canada*

Sorting of secretory cargo and retrieval of components of the biosynthetic pathway occur at the *trans*-Golgi network (TGN). The pH within the TGN is thought to be an important determinant of these functions. However, studies of the magnitude and regulation of the pH of the TGN have been hampered by the lack of appropriate detection methods. This report describes a noninvasive strategy to measure the luminal pH of the TGN in intact cells. We took advantage of endogenous cellular mechanisms for the specific retrieval of TGN resident proteins, such as TGN38 and furin, that transit briefly to the plasma membrane. Cells were transfected with chimeric constructs that contained the internalization and retrieval signals of TGN resident proteins, and a luminal (extracellular) epitope (CD25). Like TGN38 and furin, the chimeras were shown by fluorescence microscopy to accumulate within the TGN. During their transient exposure at the cell surface, the chimeras were labeled with extracellular anti-CD25 antibodies conjugated with a pH-sensitive fluorophore. Subsequent endocytosis and retrograde transport resulted in preferential labeling of the TGN with the pH-sensitive probe. Continuous, quantitative measurements of the pH of the TGN were obtained by ratio fluorescence imaging. The resting pH, calibrated using either ionophores or the "null point" technique, averaged 5.95 in Chinese hamster ovary cells and 5.91 in HeLa cells. The acidification was dissipated upon addition of concanamycin, a selective blocker of vacuolar-type ATPases. The counterion conductance was found to be much greater than the rate of H^+ pumping at the steady state, suggesting that the acidification is not limited by an electrogenic potential. Both Cl^- and K^+ were found to contribute to the overall counterion permeability of the TGN. No evidence was found for the presence of active Na^+/H^+ or Ca^{2+}/H^+ exchangers on the TGN membrane. In conclusion, selective retrieval of recombinant proteins can be exploited to target ion-sensitive fluorescent probes to specific organelles. The technique provides real-time, noninvasive, and quantitative determinations of the pH, allowing the study of pH regulation within the TGN in intact cells. The acidic pH of the TGN reflects active H^+ pumping into an organelle with a low intrinsic H^+ permeability and a high conductance to monovalent ions.

The pH prevailing in the lumen of endomembrane compartments is an important determinant of their function. The concentration of H^+ dictates the dissociation and degradation of internalized ligands (1) and modulates the processing, transport, and sorting of secreted proteins (2–4). Delivery of pH-sensitive probes by pinocytosis or receptor-mediated internalization has facilitated the study of the pH along the endocytic pathway, revealing that the acidity of the lumen increases progressively, from a pH of 6.5 to 6.0 in early and recycling endosomes to 4.5 in lysosomes (5). Conversely, the pH inside subcompartments of the secretory pathways is thought to be highest in the endoplasmic reticulum, becoming more acidic as the secretory products approach the plasma membrane. Secretory granules can attain a pH as low as ≈5.5 (6).

While the acidification is generally believed to be generated by vacuolar-type (V)[1] ATPases, the mechanisms underlying the differential pH of the individual compartments of the secretory pathway are poorly understood. This is due largely to the scarcity of appropriate methods for the determination of pH in the lumen of defined secretory compartments *in situ*. Initial studies used permeant weak bases that partition preferentially in acidic organelles, where they can be fixed and detected by immunogold (6, 7). This technique, however, is unable to provide dynamic measurements in living cells, necessary to assess the mechanisms of pH regulation. More recently, a second method was introduced that allows continuous measurement of pH in the secretory pathway. This procedure is based on the microinjection of size-fractionated liposomes (70 nm) that appear to fuse preferentially with the *trans*-Golgi cisternae (8, 9). The usefulness of this method is restricted not only by its technical complexity, but also by the fact that the pH-sensitive fluorophores delivered via liposome fusion are not retained in the *trans*-Golgi apparatus under physiological conditions, tending to move rapidly along the secretory pathway (8). A third approach has been described recently, which exploits the binding and retrograde transport of bacterial toxins to target probes to secretory organelles (10). Verotoxin was shown to accumulate and remain in the Golgi complex at physiological temperatures for a sufficient amount of time to permit adequate study of the luminal pH. Nevertheless, the precise subcompartment

* This work was supported by the Canadian Cystic Fibrosis Foundation and the Medical Research Council of Canada. The costs of publication of this article were defrayed in part by the payment of page charges. This article must therefore be hereby marked "*advertisement*" in accordance with 18 U.S.C. Section 1734 solely to indicate this fact.

§ Recipient of a Prof. Dr. Max Cloëtta fellowship.

‖ Recipient of a postdoctoral fellowship from the Medical Research Council of Canada.

‡‡ International Scholar of the Howard Hughes Medical Institute and cross-appointed to the Department of Biochemistry of the University of Toronto. To whom correspondence should be addressed: Division of Cell Biology, Hospital for Sick Children, 555 University Ave., Toronto, M5G 1X8, Canada. Tel.: 416-813-5727; Fax: 416-813-5028; E-mail: sga@sickkids.on.ca.

[1]The abbreviations used are: V, vacuolar-type; CCCP, carbonyl cyanide *m*-chlorophenylhydrazone; CHO, Chinese hamster ovary; FITC, fluorescein isothiocyanate; TGN, *trans*-Golgi network; TMA, trimethylamine.

of the Golgi apparatus targeted by the toxin remains undefined and it cannot be ruled out that verotoxin itself may influence pH homeostasis, even though its cytotoxic A subunit was omitted from the complex.

Within the secretory pathway, pH regulation is likely to be most important in the *trans*-Golgi network (TGN), where sorting of secretory cargo to different cellular destinations occurs. pH-dependent retrieval of endoplasmic reticulum components has also been shown to occur in the TGN (11). Despite its importance, the regulation of the pH in the lumen of the TGN has not been studied, due to the lack of available methods to deliver to this compartment pH-sensitive reporter molecules that are specifically targeted, well retained, and emit a continuous and quantitative signal.

The purpose of the experiments described here was to develop a strategy to measure the luminal pH of the TGN in intact, living cells by noninvasive means and to explore the determinants of acidification. We took advantage of endogenous cellular mechanisms for the specific retrieval of TGN resident proteins, such as TGN38 and furin, that transit briefly to the plasma membrane (see Fig. 1 for schematic representation of the strategy). At steady state, over 90% of these proteins is found in the TGN by virtue of a combination of retention and retrieval mechanisms (12–18). TGN38 or furin molecules that escape retention in the TGN are rapidly endocytosed and retrieved to the TGN. We reasoned that TGN proteins sojourning at the cell surface could be used to ferry fluorescent, pH-sensitive indicators back to the TGN, where they would accumulate in sufficient numbers to provide a reliable signal that could be detected by ratio imaging. This approach enabled us to analyze in some detail the mechanisms underlying the homeostasis of pH within the TGN.

EXPERIMENTAL PROCEDURES

Materials—Texas Red-labeled transferrin, BODIPY-ceramide, valinomycin, and nigericin were purchased from Molecular Probes (Eugene, OR). Brefeldin A, ATP, CCCP, and monensin were from Sigma. Concanamycin was from Kamiya Biochemical. Streptolysin O was obtained from Dr. S. Bhakdi (Johannes Gutenberg Universitat, Germany). FITC-labeled monoclonal anti-CD25 antibody was from Serotec. Butyric acid was from J. T. Baker and trimethylamine from Aldrich. All other chemicals were of analytical grade and were obtained from Fisher. Anti-calnexin antibody was the kind gift of Dr. D. Williams (University of Toronto, Canada). Antibody to α-mannosidase II was the kind gift of Dr. M. Farquhar (University of California at San Diego, CA). Cy3-labeled donkey anti-rabbit antibody was from Jackson Immunoresearch Labs. Chinese hamster ovary cells and HeLa cells were from the American Type Culture Collection (Rockville, MD).

Solutions—The Na^+-rich solution contained (in mM): NaCl 140, KCl 5, $MgCl_2$ 1, $CaCl_2$ 1, glucose 5, and Hepes 20, titrated to pH 7.3 at 37 °C. The permeabilization medium contained (in mM) K-glutamate 90, KCl 50, NaCl 10, $MgCl_2$ 1, $CaCl_2$ 2, EGTA 4, K_2HPO_4 2, and HEPES 20, titrated to pH 7.0 at 37 °C. When indicated, Cl^- was replaced isoosmotically with glutamate$^-$, and K^+ was replaced with the appropriate salt of Na^+ or *N*-methyl-D-glucammonium+.

Cells—Chinese hamster ovary cells were transfected with a plasmid encoding a chimeric protein composed of the extracellular domain of CD25 and the transmembrane and cytoplasmic domains of rat TGN38 (CD25-TGN38 construct). Details of the DNA recombination procedures used to generate this construct can be found in Humphrey *et al.* (13). To select stable transfectants, cells plated on 12-well plates were co-transfected with 15 μg of CD25-TGN38 and 5 μg of pcDNA3 (to confer resistance to geneticin) by the calcium phosphate precipitation method. Cells were incubated in culture medium for 24 h before selection of stable expressors. Cells expressing CD25-TGN38 stably were selected by incubation for 14 days in medium containing 0.25 mg/ml geneticin (G418; Life Technologies, Inc., Burlington, Ontario, Canada). Clonal lines were selected and expanded in medium fortified with 0.1 mg/ml G418. Expression of the chimeric protein was assessed by staining fixed and permeabilized cells with fluorescein-coupled rat anti-CD25 antibody, as detailed below.

HeLa cells were transfected transiently with plasmids encoding either CD25-TGN38 or a chimeric protein composed of the extracellular domain of CD25 and the transmembrane and cytoplasmic domains of furin (CD25-furin construct). Details of the construction of CD25-furin can be found in (15). The transfected cells were grown in α-minimal essential medium (Ontario Cancer Institute, Toronto) supplemented with 10% fetal calf serum and 1% antibiotic solution (penicillin and streptomycin, Life Technologies, Inc.). For immunofluorescence or video imaging, the cells were plated on glass coverslips for 24–48 h before the experiment.

Epifluorescence and Confocal Microscopy—Cells were fixed with 4% paraformaldehyde, permeabilized with 0.1% Triton X-100, and incubated for 1 h with either 1:200 anti-calnexin antibody or 1:500 anti-α-mannosidase II antibody, and then for 1 h with 1:1500 Cy3-labeled donkey anti-rabbit antibody. Images were acquired on a Leica TCS 4D laser confocal microscope, using a 63× objective and fluorescein or rhodamine filter combinations. Digital images were assembled and labeled using Adobe Photoshop (Adobe Systems Inc.) and Microsoft PowerPoint software.

To stain the TGN, cells were incubated with 20 μg/ml BODIPY-ceramide for 20 min at 37 °C, washed, chased in phosphate-buffered saline for 20 min at 37 °C, and immediately visualized using a Leica DM-IRB microscope equipped with a Micromax cooled charge-coupled device camera (Princeton Instruments, Trenton, NJ), operated from a Dell computer using Winview software (Princeton Instruments). Recycling endosomes were visualized using the same system, after allowing internalization of Texas Red-labeled transferrin (20 μg/ml) for 30–45 min at 37 °C.

pH Imaging—Ratio fluorescence imaging was performed on a Zeiss Axiovert 100 TV inverted microscope (Zeiss, Germany) using a NeoFluar 63×/1.25 numerical aperture objective, as described previously (19). Fluorescence image pairs at 490 and 440 nm excitation were captured at 120-s intervals using 300-ms exposure and 4 × 4 pixel binning to increase sensitivity.

Image Processing—The 490 and 440 nm fluorescence images were corrected for shading to compensate for uneven illumination, the background was subtracted, and a threshold of 5 times the value of the background noise (root mean square) was applied before obtaining a pixel-by-pixel ratio of the two images. Subthreshold pixels were neither displayed nor used for subsequent analysis, to prevent artifacts caused by ratioing near-zero values. The resulting ratio images were displayed on-line, and regions of interest encompassing the TGN structures were defined. The averaged ratio values of the regions of interest were calculated and plotted to follow the kinetics of the pH changes throughout an experimental period.

Calibration—Two independent methods of calibration were used. At the end of each experiment, a calibration curve of fluorescence ratio *versus* pH was obtained *in situ* by sequential perfusion with KCl-rich medium containing 5 μg/ml nigericin plus 5 μM monensin, buffered at four different pH values, according to Thomas *et al.* (20). This calibration procedure was validated by the null point method (21) using solutions containing varying ratios of butyric acid and trimethylamine (TMA), plus 50 mM NaCl and 20 mM HEPES, pH 7.2. The concentrations of butyric acid and TMA (in mM) and the calculated null pH were: 40/40 (pH = 6.3), 73/7.3 (pH = 5.8), and 80/0.8 (pH 5.3).

Data Analysis and Statistics—Quantification of cell-associated fluorescence was performed using the Metamorph/Metafluor package (Universal Imaging, West Chester, PA). Data were graphed using the Origin software (MicroCal Software Inc., Northampton, MA) and are shown as means ± 1 S.E.

RESULTS

Strategy—As described in the Introduction, the retrograde transport of TGN-resident proteins was harnessed to target fluorescent, pH-sensitive probes to the lumen of the TGN (Fig. 1). The probe of choice was fluorescein, which has a high quantum yield and a pK_a of ≈6.5, providing optimal sensitivity in the mildly acidic pH range expected for secretory organelles. Our strategy involved binding of fluoresceinated antibodies to the extracellular (luminal) domain of TGN-localized proteins during their transient exposure at the surface membrane. To facilitate delivery of fluoresceinated antibodies to the TGN, we generated chimeric proteins that retain the transmembrane and cytosolic regions of TGN38 or furin, including the determinants of TGN targeting, but replaced the extracellular domain by that of CD25, the α-chain of the interleukin-2 receptor (Fig.

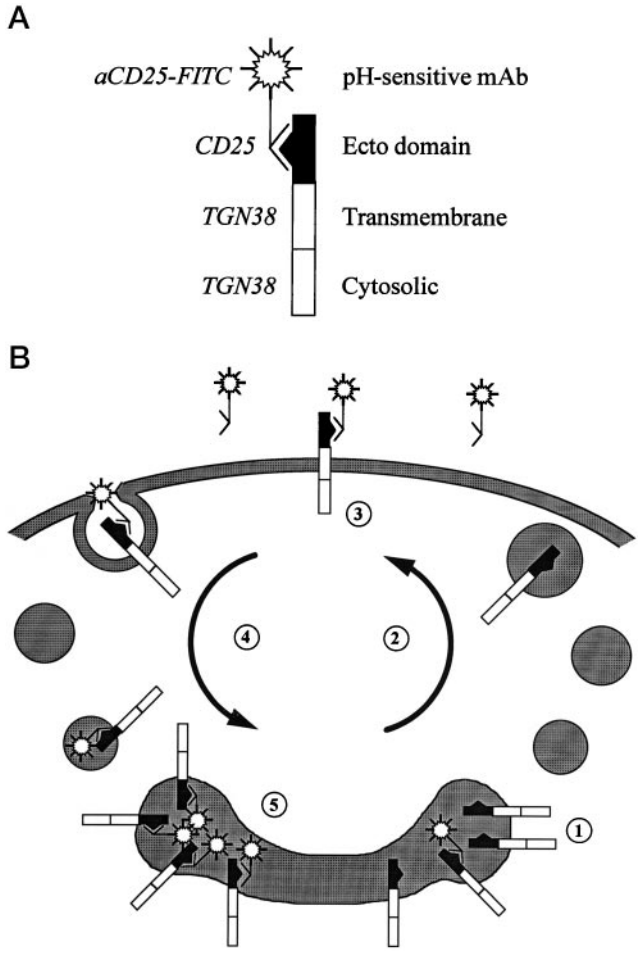

FIG. 1. **Targeting probes to the TGN.** *A*, the targeting chimeric protein was constructed by attaching the ectodomain of CD25 to the transmembrane and cytosolic domains of TGN38. CD25 is recognized by an FITC-labeled monoclonal antibody. The fluorescein moiety serves as a probe for intracellular pH measurements. *B*, transfected cells express the chimeric protein predominantly in the TGN (*1*). Cycling of the protein between the TGN and the plasma membrane (*2*) exposes the CD25 epitope extracellularly and allows binding of the fluorescent antibody (*3*). Retrograde transport of the tagged protein (*4*) results in the eventual accumulation of fluorophore in the TGN (*5*) providing a means to selectively measure the pH of this compartment.

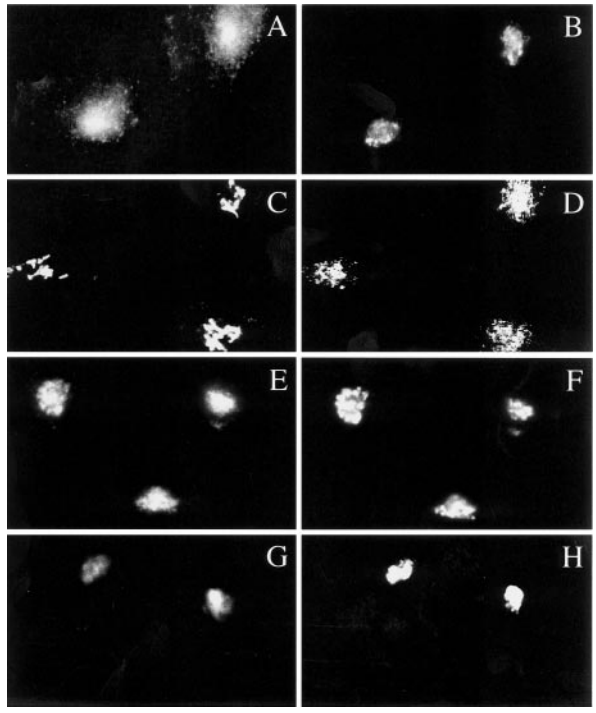

FIG. 2. **Immunolocalization of the internalized CD25-TGN 38 chimera in stable transfectants.** CHO cells were stably transfected with the CD25-TGN38 construct and allowed to internalize the FITC-labeled anti-CD25 antibody overnight. *A*, staining of recycling endosomes with Texas Red-conjugated transferrin; *B*, distribution of the CD25-TGN38 chimera in the same cells shown in *A*, as visualized using anti-CD25 antibody; *C*, staining of the Golgi cisternae with anti-α-mannosidase II antibodies; *D*, distribution of the CD25-TGN38 chimera in the same cells shown in *C*; *E*, staining of the TGN with BODIPY-ceramide; *F*, distribution of the CD25-TGN38 chimera in the same cells shown in *E*; *G*, staining of the TGN with BODIPY-ceramide in cells pretreated with 5 μg/ml brefeldin A for 2 h at 37 °C; *H*, distribution of the CD25-TGN38 chimera in the same cells shown in *E*. Images are representative of at least three experiments of each type. *C* and *D* are confocal images. All others are epifluorescence images captured with a cooled charge-coupled device camera, as described under "Experimental Procedures."

1*A*). This protein was chosen because of the availability of highly specific, fluoresceinated monoclonal antibodies. Such chimeric proteins had been shown earlier to accumulate in the TGN and recycle via the plasma membrane (Fig. 1*B*) in a manner similar to the endogenous TGN-resident proteins (13, 15, 17, 18). We therefore anticipated that incubation of live cells expressing the chimeras with anti-CD25 antibodies would result in gradual accumulation of the pH-sensitive moiety, fluorescein, in the TGN (Fig. 1*B*).

Subcellular Distribution of the Chimeric Constructs—Chinese hamster ovary cells were transfected stably with the CD25-TGN38 construct and incubated overnight with the fluorescein-conjugated anti-CD25 antibody at 37 °C. The localization of the internalized antibody was evaluated by fluorescence microscopy. As shown in Fig. 2, *B*, *D*, and *F*, the anti-CD25 antibodies accumulated in a juxtanuclear structure, with a minor fraction distributing more peripherally in small vesicular structures. Dual labeling indicated that the site of accumulation of the chimeric proteins is not the endoplasmic reticulum, identified using anti-calnexin antibodies (not illustrated). The juxtanuclear structures containing the CD25 antibody were in the vicinity of, but distinct from recycling endosomes, labeled by a 30–45-min incubation with Texas Red-conjugated transferrin (Fig. 2, *A* and *B*). Similarly, the CD25-TGN38 chimera was found to localize in a compartment that was closely apposed, but distinguishable from the medial Golgi cisternae, revealed by anti-α-mannosidase II antibodies (*cf.* Fig. 2, *C* and *D*). Instead, the chimeric protein was found to co-localize precisely with a fluorescent ceramide derivative (Fig. 2, *E* and *F*), known to accumulate in the TGN (22). That the chimera is located in the TGN and not the Golgi cisternae is also suggested by experiments using brefeldin A. This fungal metabolite is known to promote retrograde fusion of the cisternae with the endoplasmic reticulum, while inducing the collapse of the TGN into a tight tubulovesicular complex (23, 24). As shown in Fig. 2*H*, the fluorescence of the anti-CD25 antibody did not disperse to a reticular pattern but instead coalesced into a juxtanuclear complex, as did the ceramide derivative (Fig. 2*G*). Taken together, these findings strongly suggest that the CD25 antibody is concentrated in the TGN, validating the use of retrograde transport to deliver pH-sensitive probes to this organelle.

pH Calibration—Fig. 3*A* demonstrates that the fluorescence of the internalized antibody is sensitive to the surrounding pH. The pH of the lumen was manipulated by addition of the cation/H^+ exchange ionophores nigericin and monensin, while bathing the cells in K^+-rich media of varying pH. Fluorescence images were captured sequentially with excitation at 490 and

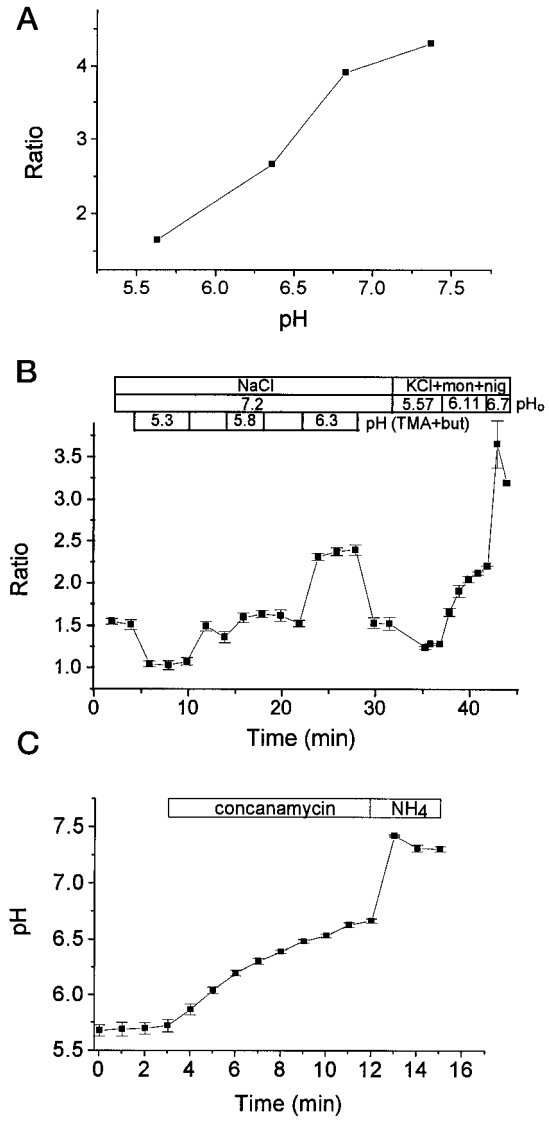

FIG. 3. ***In situ* pH measurements and calibration.** *A*, dependence of the fluorescence ratio on pH. The TGN was labeled with anti-CD25 antibodies as described in Fig. 1 and the pH was clamped using K^+-based solutions containing the ionophores nigericin and monensin. The excitation ratio (490/440 nm) of the FITC fluorescence emitted by the juxtanuclear structures was plotted against the pH of the calibration media. *B*, fluorescence ratio was measured dynamically during sequential perfusion with Na^+-based solutions containing varying concentrations of butyrate (*but*) and TMA. The pH at which each combination is predicted to equilibrate is indicated in the *lower bar*. Where indicated, monensin (*mon*) and nigericin (*nig*) were added in K^+-rich media of the indicated extracellular pH (pH_o; *middle bar*). Data are means ± S.E. of eight cells from a typical experiment out of four. *C*, the pH of the TGN was measured in cells bathed in Na^+-rich solution. Where indicated, concanamycin (50 nM) and NH_4Cl (10 mM) were added to the solution. Data are means ± S.E. of four cells from a typical experiment out of four.

440 nm under each condition, and individual TGN structures were outlined on the ratio image. As illustrated in Fig. 3*A*, the 490/440 nm fluorescence ratio varies markedly with pH in the range of 5.5 to 7.5. The behavior of the dye *in situ* was indistinguishable from that observed *in vitro* (not shown), implying that its fluorescence properties were not affected by the microenvironment of the TGN. If one assumes that in the presence of the ionophores the pH of the TGN becomes identical to that of the extracellular medium (20), this approach can be used to provide an absolute calibration of the pH of the TGN in the steady state (Fig. 3*B*). In 110 cells, the resting pH of the TGN was estimated to be 5.95 ± 0.03 (mean ± S.E.; range, ≈5.7–6.4) using the ionophore calibration procedure.

Calibration using exchange ionophores rests on the assumption that the monovalent cation activity inside the TGN is comparable to that in the surrounding medium and that the amounts of cations transported during the transitions between pH values affect their concentration negligibly. Departures from these assumptions would produce systematic errors in the calibration, as has been recently shown to occur in measurements of the cytosolic pH (25). Because the ionic composition of the TGN has not been well defined, we implemented a second calibration procedure, which is independent of the transport of Na^+ and K^+. This approach uses varying ratios of weak acids and bases to search for a null point where the rates of protonation/deprotonation of the permeant species of the weak electrolytes are identical. For a given combination of acid and base, the null point is strictly a function of the luminal pH of the compartment under investigation (21). The cells were therefore sequentially perfused with solutions containing varying concentrations of butyrate and TMA, while keeping the osmolarity and the extracellular pH constant (see "Experimental Procedures"). The ratio of fluorescence in the TGN was measured throughout, to detect the null point pH (Fig. 3*B*). Acid/base combinations expected to equilibrate at pH of 5.3 and 6.3 induced departures of the ratio in the acidic and alkaline direction, respectively, suggesting that the TGN has an intermediate pH. Accordingly, exposure to a solution with predicted equilibrium at pH of 5.8 had virtually no effect on the fluorescence ratio and thus approximated the null point (Fig. 3*B*). This value corresponded well to the value obtained by subsequent calibration of the same cells with nigericin/monensin (Fig. 3*B*). A good correspondence between the two methods was obtained in three separate experiments, thus validating the calibration with ionophores.

It was important to ascertain that the results obtained with stably transfected CHO cells were not unique to the clone selected or to the chimeric construct used to target the TGN. To obtain independent measurements of the pH of the TGN, we therefore used a second cell line and compared two different constructs. HeLa cells were transiently transfected with either the CD25-TGN38 chimera or with an analogous CD25-furin construct, using the calcium phosphate precipitation method. Typical results are shown in Fig. 4. The distribution of the chimeras within the cells was more heterogeneous in the transient transfectants than in the stable CHO clones. In addition to juxtanuclear accumulation close to the Golgi cisternae (*cf.* Fig. 4, *A* and *B*), cells showing the highest level of expression displayed also more disperse punctate fluorescence throughout the cell. Delocalization associated with overexpression of TGN resident proteins had been reported earlier (13, 26) and likely reflects saturation of the receptors that target the chimeras to the TGN. Despite the occurrence of occasional delocalization, the pH of the juxtanuclear fluorophore could be studied in isolation either by studying preferentially cells with moderate levels of expression, where targeting was specific, and/or by defining "regions of interest" within the cell that encompassed only the site of pericentriolar fluorescence, using the Metafluor software. As in the case of CHO cells, the TGN of HeLa cells was acidic and was dissipated by addition of weak bases (Fig. 4*C*). In 38 determinations, the pH of the TGN in HeLa cells averaged 5.91 ± 0.05. Results obtained using the TGN38 and furin chimeras were indistinguishable.

Evidence for Vacuolar ATPase Activity in the TGN—In other compartments of the secretory pathway, luminal acidification is due primarily to H^+ pumping by ATPases (3, 27). A similar mechanism appears to be at work in the TGN. As shown in

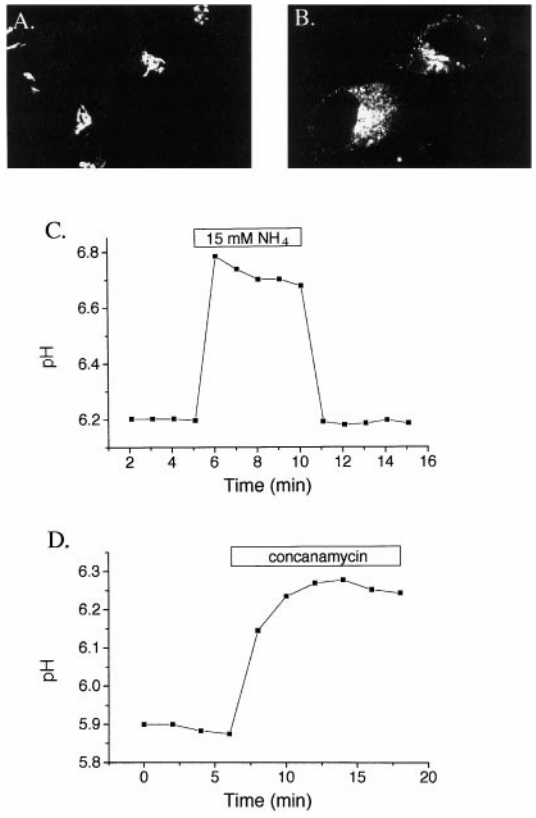

FIG. 4. **Distribution of CD25-TGN38 and pH measurements in HeLa cells.** HeLa cells were transiently transfected with the CD25-TGN38 construct, grown on glass coverslips for 48 h, and incubated overnight with anti-CD25 antibody. *A*, confocal image showing immunolocalization of α-mannosidase II in HeLa cells. *B*, localization of CD25-TGN38 in the same cells shown in *A*. *C*, the pH of the TGN of HeLa cells was measured as in Fig. 3. Where indicated, 15 mM NH_4Cl was added to the medium; *D*, effect of concanamycin (50 nM) on the steady-state pH of the TGN of transiently transfected HeLa cells. Traces in *C* and *D* are representative of four experiments.

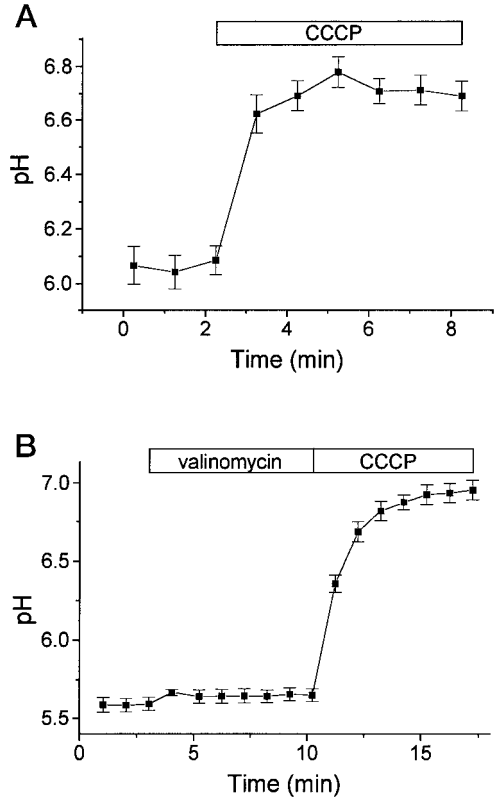

FIG. 5. **Effects of ionophores on the pH of the TGN.** *A*, the pH of the TGN was measured in CHO cells bathed in Na^+-rich solution, as in Fig. 3*C*. Where indicated, 2 μM CCCP was added to the bathing medium. Data are means ± S.E. of 11 cells from a typical experiment out of three. *B*, the pH of the TGN of CHO cells was measured as above. Where indicated, valinomycin (1 μM) and CCCP (2 μM) were added sequentially to the solution. Data are means ± S.E. of 13 cells from a typical experiment out of three.

Figs. 3*C* and 4*D*, the steady state acidification of the TGN is dissipated upon addition of concanamycin, a potent and specific inhibitor of V-ATPases (28). Similar results were obtained using another V-ATPase inhibitor, namely bafilomycin A_1 (not illustrated). These agents did not alter the morphology (not shown) or compromise the integrity of the TGN, as indicated by the alkalinization induced by the subsequent addition of ammonium (Fig. 3*C*). These findings indicate that maintenance of the acidic pH of the TGN requires continuous H^+ pumping, to offset the sizable "leak" that is manifested upon addition of concanamycin.

Because the behavior of transfected HeLa and CHO cells was similar and considering the tighter pericentriolar localization of the label in the latter cells, all subsequent experiments were performed with the stably transfected CHO cells.

Passive H^+ Permeability—Dissipation of the pH gradient upon addition of concanamycin occurred relatively slowly, requiring over 10 min to reach completion (Fig. 3*C*). This could be the result of a limited permeability to H^+ (equivalents) or of a low counterion conductance. These alternatives could be resolved using the H^+-specific ionophore CCCP. If the movement of counterions restricts the rate of H^+ efflux, further increasing the H^+ conductance by adding the protonophore is expected to have little effect on the rate of pH change. As illustrated in Fig. 5, addition of CCCP yielded a very rapid alkalinization that equilibrated within 3 min. Notice that, unlike Fig. 3*C*, the pH dissipation induced by the protonophore occurred in the absence of concanamycin. The presence of active pumps may account for the slightly acidic pH attained in the steady state.

These observations imply that the endogenous H^+ permeability limits the rate of dissipation and that the counterion conductance is high. In accordance with this conclusion, addition of the K^+ ionophore valinomycin had little effect on the resting pH of the TGN and only marginally increased the rate of CCCP-induced dissipation (Fig. 5*B*). The failure of valinomycin to alter the resting pH also suggests that the rate of H^+ pumping is not limited by the movement of counterions.[2] Because similar observations were made increasing H^+ permeability with FCCP and dinitrophenol (not illustrated), it is unlikely that the counterion conductance is increased by the protonophores themselves.

Characterization of Counterion Permeability—The experiments using ionophores led to the conclusion that the movement of charge compensating ions does not limit the pumping or leakage of H^+. This conclusion is unexpected, since it had been proposed that the differential pH of individual compartments of the secretory pathway was attributable to their limited counterion conductance (29). The nature of the pathways mediating the large counterion permeability of the TGN and their role in the establishment of the acidification was investigated next. This required rapid and thorough substitution of

[2] This tentative conclusion is based on the assumption that the K^+ concentration of the TGN is high. This assumption is likely valid (Fig. 3*B*). Moreover, following dissipation of the luminal acidification with CCCP, addition of valinomycin had no detectable effect on the pH (not illustrated). Because the TGN pH equilibrated near the cytosolic pH, this suggests that the luminal and cytosolic concentrations of K^+ are very similar.

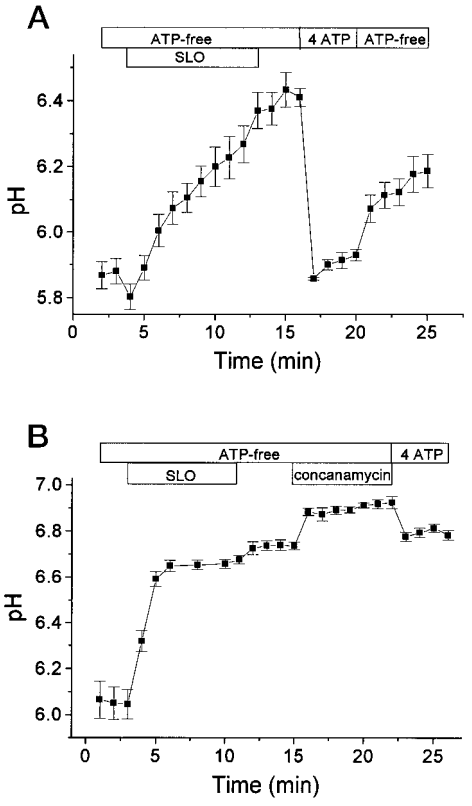

FIG. 6. **Acidification of the TGN is ATP-dependent and concanamycin-sensitive.** The TGN of CHO cells was stained with FITC-labeled anti-CD25, as described in Fig. 1. The cells were then bathed in K^+-glutamate-based solution devoid of exogenous ATP and, where indicated, the plasma membrane was permeabilized with streptolysin O (*SLO*) (0.5 μg/ml). *A*, where indicated 4 mM ATP was reintroduced to the bathing medium and then withdrawn again. Data are means ± S.E. of six cells from a typical experiment out of four. *B*, where noted, the cells were treated with 50 nM concanamycin and then ATP (4 mM) was reintroduced. Data are means ± S.E. of five cells from a typical experiment out of four.

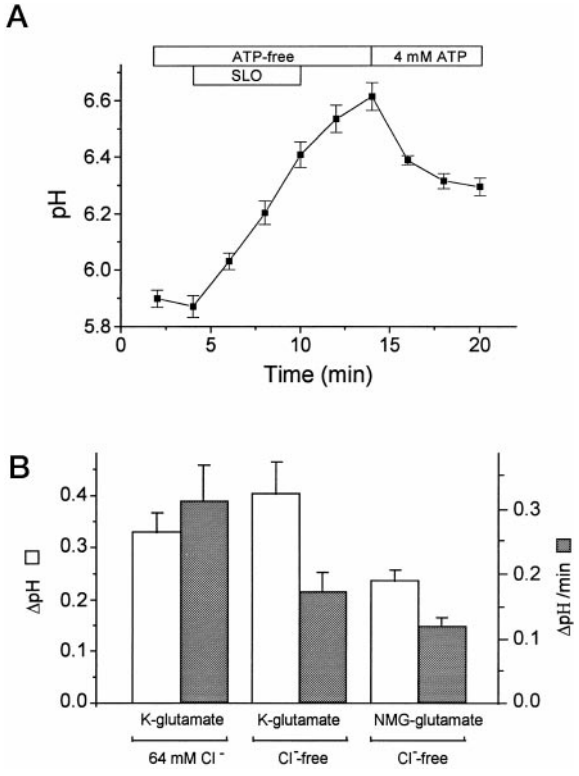

FIG. 7. **Assessment of counterion conductance.** *A*, the TGN of CHO cells was stained with FITC-labeled anti-CD25, as described in Fig. 1. The cells were then bathed in Cl^--free, *N*-methyl-D-glucammonium glutamate-based solution devoid of exogenous ATP and, where indicated, the plasma membrane was permeabilized with streptolysin O (0.5 μg/ml). Finally, ATP (4 mM) was re-added. Data are means ± S.E. of four cells from a typical experiment out of four. *B*, summary of studies such as that illustrated in *A*, using permeabilization media of varying composition. Leftmost bars: K^+-glutamate medium containing Cl^-. *Middle bars*, Cl^--free K^+-glutamate solution. *Rightmost bars*, Cl^--free *N*-methyl-D-glucammonium (*NMG*) glutamate. The maximal ΔpH attained upon reintroduction of ATP is shown by *open bars*. The maximal rate of acidification recorded upon addition of ATP is shown by the *stippled bars*. Data are means ± S.E. of four experiments.

the ionic composition of the milieu bathing the TGN, *i.e.* the cytosol. To this end, we implemented a system where the plasmalemma was selectively permeabilized with streptolysin O, under conditions where the TGN membrane remained intact. Effective permeabilization of the plasmalemma by streptolysin O was demonstrated by staining of the cells with trypan blue and propidium iodide (not shown) and by the sudden alkalinization of the TGN observed when permeabilization took place in media devoid of ATP (Fig. 6*A*). The dissipation of the pH gradient was due to washout of cytosolic ATP and not to damage of the TGN membrane, since re-introduction of exogenous ATP (4 mM) induced the rapid restoration of the original, acidic pH (Fig. 6*A*). The very rapid re-acidification of the TGN was mediated by the V-ATPase, since it was virtually eliminated by pretreatment with concanamycin, a poorly reversible inhibitor (Fig. 6*B*).

Measurement of the acidification induced by re-addition of ATP to permeabilized cells provided a convenient procedure to study the charge-compensating mechanism. Under such conditions, substantial movement of counterions must occur to neutralize the high rate of H^+ translocation. Therefore, systematic replacement of the major ions in the permeabilization medium by impermeant substituents was performed to define their contribution to charge neutralization. As shown in Fig. 7*A*, substitution of K^+ and Cl^- by larger, purportedly impermeant ions (*N*-methyl-D-glucammonium$^+$ and glutamate$^-$) markedly reduced the rate of H^+ pumping. The steady state pH attained under these conditions was also less acidic than in the presence of K^+ and Cl^- (Fig. 7*B*). Replacement of Cl^-, while maintaining a normal concentration of K^+, reduced the rate of acidification by nearly 50%, but did not affect the final steady-state pH (Fig. 7*B*). Thus, K^+ can sustain full acidification of the TGN in the nominal absence of Cl^-, though at reduced rates. Replacement of cytosolic K^+ by NMG^+ likely leads to depletion of luminal K^+, accounting for the observed inhibition. We conclude that both influx of anions and efflux of cations from the TGN can compensate for the net charge translocated inward by the V-ATPase. It must be borne in mind, however, that inorganic anions have been reported to exert allosteric effects on the ATPase (30). We therefore cannot rule out that this effect contributes to the inhibition observed upon Cl^- removal.

Assessment of the Presence of Na^+/H^+ and Ca^{2+}/H^+ Exchangers—Plasma membrane H^+ transporters such as the ubiquitous Na^+/H^+ exchanger transit through the Golgi *en route* to their final destination. It is not clear whether during biosynthetic transit they are functional and capable of mediating significant H^+ fluxes across the membrane of the TGN. Na^+/H^+ exchange in mammalian cells is electroneutral and bidirectional, and elevation of the cytosolic Na^+ would tend to dissipate the acidic pH of organelles by driving the efflux of luminal H^+. To test for the presence of Na^+/H^+ exchange, we measured the pH of the TGN in cells permeabilized with streptolysin O and varied the concentration of Na^+ in the medium (Fig. 8). Using K^+, the main cationic constituent of normal

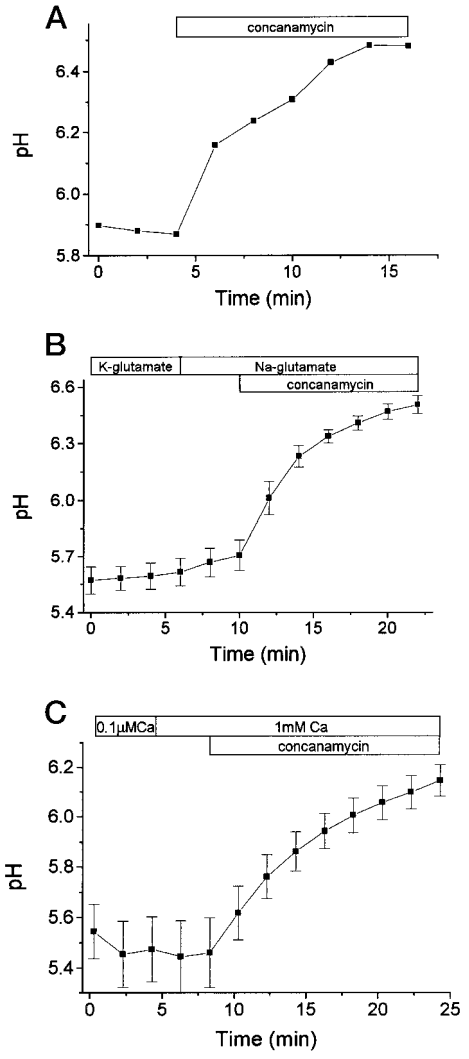

FIG. 8. **Effect of increased cytosolic Na^+ and Ca^{2+} on the pH of the TGN.** The TGN of CHO cells was stained with FITC-labeled anti-CD25, as in Fig. 1. The cells were then bathed in K^+-glutamate-based solution with Cl^- in the presence of ATP/Mg and the plasma membrane was permeabilized with streptolysin O (0.5 μg/ml). Traces start after permeabilization was completed. *A*, where indicated, 50 nM concanamycin was added; *B*, permeabilized cells were initially perfused with normal K^+-glutamate medium. Where indicated, the medium was replaced by a Na^+-rich glutamate medium. Finally, concanamycin was added. Data are means ± S.E. of five cells from a typical experiment out of three. *C*, permeabilized cells were initially perfused with normal K^+-glutamate medium, which contains ≈0.1 μM free calcium. Where indicated, the concentration of free calcium was raised to 1 mM. Finally, concanamycin was added. Data are means ± S.E. of three cells from a typical experiment out of three.

cytosol, as the major cation in the permeabilization medium, we found the resting pH of the TGN to be sustained and comparable to that of intact cells, provided ATP/Mg was present throughout (Fig. 8*A*). As expected, the transmembrane pH gradient was rapidly dissipated by concanamycin. Replacement of cytosolic K^+ by Na^+ induced a very slight alkalinization of the resting pH of the TGN (Fig. 8*B*), suggesting that Na^+/H^+ exchange activity is minute. We considered the possibility that concomitant activation of the V-ATPase would offset the H^+ efflux mediated by Na^+/H^+ exchange. This possibility was not substantiated experimentally, since the rates of concanamycin-induced dissipation were comparable in K^+-rich and Na^+-rich cytosolic media (*cf.* Fig. 8, *A* and *B*). Jointly, these observations imply that Na^+/H^+ exchange does not contribute importantly to transmembrane H^+ fluxes in the TGN.

Ca^{2+}/H^+ exchange is known to operate across the inner mitochondrial membrane in mammalian cells. In addition, Ca^{2+}/H^+ exchangers have been described in yeast vacuoles (31) and in the acidic organelles of trypanosoma (32). To assess the presence of this exchanger in the TGN membrane, the concentration of Ca^{2+} in the permeabilization solution was rapidly stepped up from its basal level of 0.1 μM to 1 mM. As shown in Fig. 8*C*, this maneuver had little effect on either the resting pH or on the rate of concanamycin-induced dissipation. Thus, under the conditions of our experiments, Ca^{2+}/H^+ exchange activity was not detectable in the TGN membrane.

DISCUSSION

We describe here a convenient method to measure the pH of the TGN in intact cells, using an endogenous retrograde pathway to transport specifically to this organelle recombinant proteins tagged with ion-sensitive fluorescent probes. This technique provides real time, noninvasive, and quantitative determinations of the pH of the TGN, allowing physiological measurements in living cells. It represents an improvement over previous methods for the measurement of pH in the secretory pathway in at least two respects. Unlike the liposome fusion and toxin internalization methods, the probe is targeted to a single, well defined subcompartment of the Golgi complex, namely the TGN. Second, following equilibration with the labeled antibody, the location of the probe remains constant for very extended periods under physiological conditions. Fluid phase probes delivered via liposomes move rapidly forward along the secretory pathway (8, 9), whereas verotoxin gradually moves retrogradely (10), ultimately reaching the endoplasmic reticulum.

The preferential accumulation of the probe in the TGN was confirmed by dual labeling with specific organellar markers, and ratio imaging was used to obtain quantitative pH measurements, which were calibrated *in situ* by two independent methods. Using this technique, the resting TGN pH averaged 5.95 in CHO cells and 5.91 in HeLa cells. These values are significantly more acidic than those reported for the Golgi cisternae by Seksek *et al.* (8, 9) and by Kim *et al.* (10), which ranged between ≈6.2 and 6.6. This observation is consistent with earlier electron microscopic measurements using 3-(2,4-dinitroanilino)-3′-amino-*N*-methyldipropylamine, showing that the distal subcompartments of the Golgi complex become progressively more acidic (6). A low pH in the lumen of the TGN is thought to be important to promote coupling of KDEL-containing proteins with their receptors, for sorting of cargo to different destinations, in part by local segregation of glycolipid rafts, and for other functions.

The differential pH of individual subcellular compartments has been attributed to varying counterion permeability (29). This hypothesis implies that, at the steady state, pumping by V-ATPases is at or very near thermodynamic equilibrium and that the sum of the chemical and electrical components to the proton-motive force dictate the pH. This condition is unlikely to apply to the TGN, since reducing the electrical component by addition of conductive ionophores had no discernible effect on pH. Moreover, the comparatively rapid dissipation of pH upon addition of concanamycin implies that a sizable H^+ leak exists, which likely prevents the pump from approaching thermodynamic equilibrium. Finally, the accelerated dissipation induced by CCCP implies that the conductance of the charge-compensating ions is greater than that of the endogenous leak, which at steady state must be identical to the rate of pumping. For these reasons, we feel that the counterion conductance is not likely to be a defining factor of the pH of the TGN.

Alternatively, the number or kinetic properties of the V-ATPases in different compartments could account for their

unique pH. Two distinct isoforms of the 100-kDa subunit have been reported to co-exist in different organelles in yeast (33, 34). In addition, isoforms of some of the subunits have been described in different animal tissues (*e.g.* see Ref. 35). However, there are, to our knowledge, no reports of differential distribution of isoenzymes among endomembrane compartments of a single mammalian cell. Therefore, differences in the abundance of pumps or of the leak pathways that counteract their effects are, at present, the most likely explanation for the heterogeneity of the pH of individual subcompartments of the Golgi apparatus. In this regard it is noteworthy that the rate of pH dissipation following inhibition of the pump was greater in the Golgi cisternae (10) than found here for the TGN (*e.g.* Fig. 3), correlating well with the greater acidity of the latter compartment.

The nature of the leak pathways remains undefined. We ruled out a significant contribution by Na^+/H^+ or Ca^{2+}/H^+ exchangers like those described in the plasma membrane and in other organelles. Moreover, our experiments were carried out in nominally HCO_3^--free media, so that exchange of Cl^- for HCO_3^- is also unlikely. Other possibilities include H^+ antiports or symports intended to drive the uptake of substrates or the export of metabolites, respectively, or proton conductive "channels" like those described in the plasma membrane of some specialized cells (36, 37). Regardless of their precise identity, the H^+ efflux pathways of intracellular organelles may be an important determinant of their steady state pH and therefore of their functional properties.

REFERENCES

1. Mellman, I., Fuchs, R., and Helenius, A. (1986) *Annu. Rev. Biochem.* **55,** 663–700
2. Orci, L., Ravazzola, M., Amherdt, M., Madsen, O., Perrelet, A., Vassalli, J. D., and Anderson, R. G. (1987) *J. Cell Biol.* **103,** 2273–2281
3. Mellman, I. (1992) *J. Exp. Biol.* **172,** 39–45
4. Carnell, L., and Moore, H.-P. (1994) *J. Cell Biol.* **127,** 693–705
5. Maxfield, F. R., and Yamashiro, D. J. (1991) *Intracellular Trafficking of Proteins*, pp. 157–182, Cambridge University Press, Cambridge, UK
6. Anderson, R. G., and Pathak, R. K. (1985) *Cell* **40,** 635–643
7. Orci, L., Ravazzola, M., and Anderson, R. G. (1987) *Nature* **326,** 77
8. Seksek, O., Biwersi, J., and Verkman, A. S. (1995) *J. Biol. Chem.* **270,** 4967–4970
9. Seksek, O., Biwersi, J., and Verkman, A. S. (1996) *J. Biol. Chem.* **271,** 15542–15548
10. Kim, J. H., Khine, A. A., Lingwood, C. A., Furuya, W. F., Manolson, M. F., and Grinstein, S. (1996) *J. Cell Biol.* **134,** 1387–1399
11. Miesenböck, G., and Rothman, J. E. (1995) *J. Cell Biol.* **129,** 309–319
12. Bos, K., Wright, C., and Stanley, K. K. (1993) *EMBO J.* **12,** 2219–2228
13. Humphrey, J. S., Peters, P. J., Yuan, L. C., and Bonifacino, J. S. (1993) *J. Cell Biol.* **120,** 1123–1135
14. Wong, S. H., and Hong, W. (1993) *J. Biol. Chem.* **268,** 22853–22862
15. Bosshart, H., Humphrey, J., Deigman, E., Davidson, J., Drazba, J., Yuan, L. C., Oorschot, V., Peters, P. J., and Bonifacino, J. S. (1994) *J. Cell Biol.* **126,** 1157–1172
16. Molloy, S. S., Thomas, L., van Slyke, J. K., Stenberg, P. E., and Thomas, G. (1994) *EMBO J.* **13,** 18–33
17. Rajasekaran, A. K., Humphrey, J. S., Wagner, M., Miesenböck, G., Le Bivic, A., Bonifacino, J. S., and Rodriguez-Boulan, E. (1994) *Mol. Biol. Cell* **5,** 1093–1103
18. Voorhees, P., Deignan, E., Humphrey, J., Marks, M. S., Peters, P. J., and Bonifacino, J, S. (1995) *EMBO J.* **14,** 4961–4975
19. Demaurex, N., Waddell T., Downey G. P., and Grinstein S.(1996) *J. Cell Biol.* **133,** 1–13
20. Thomas, J. A., Buchsbaum, R. N., Zimniak, A., and Racker, E. (1982) *Biochemistry* **18,** 2210–2218
21. Eisner, D. A., Kenning, N. A., O'Neill, S. C., Pocock, G., and Valdeolmillos, M. (1989) *Eur. J. Physiol.* **413,** 553–558
22. Pagano, R. E., Sepanski, M. A., and Martin, O. C. (1989) *J. Cell Biol.* **109,** 2067–2079
23. Lippincott-Schwartz, J., Yuan, L. C., Bonifacino, J. S., and Klausner, R. D. (1989) *Cell* **56,** 801–813
24. Wood, S. A., Park, J. E., and Brown, W. J. (1991) *Cell* **67,** 591–600
25. Boyarsky, G., Hanssen, C., and Clyne, L. A. (1996) *FASEB J.* **10,** 1205–1212
26. Ponnambalam, S., Rabouille, C., Luzio, J. P., Nilsson, T., and Warren, G. (1994) *J. Cell Biol.* **125,** 253–268
27. Forgac, M. (1992) *J. Bioenerg. Biomembr.* **24,** 341–350
28. Woo, J. T., Shinohara, C., Sakai, K., Hasumi, K., and Endo, A. (1992) *Eur. J. Biochem.* **207,** 383–389
29. Al-Awqati, Q., Barasch, J., and Landry, D. (1992) *J. Exp. Biol.* **172,** 245–266
30. Moriyama, Y., and Nelson, N. (1987) *J. Biol. Chem.* **262,** 14723–14729
31. Pozos, T. C., Sekler, I., and Cyert, M. C. (1996) *Mol. Cell. Biol.* **16,** 3730–3741
32. Vercesi, A. E., Moreno, S. N., and Docampo, R. (1994) *Biochem. J.* **304,** 227–233
33. Manolson, M. F., Proteau, D., Preston, R. A., Stenbit, A., Roberts, B. T., Hoyt, M. A., Preuss, D., Mulholland, J., Botstein, D., and Jones, E. W. (1992) *J. Biol. Chem.* **267,** 14294–14303
34. Manolson, M. F., Wu, B., Proteau, D., Taillon, B. E., Roberts, B. T., Hoyt, M. A., and Jones, E. W. (1992) *J. Biol. Chem.* **269,** 14064–14074
35. Nelson, R. D., Guo, X. L., Masood, K., Brown, D., Kalkbrenner, M., and Gluck, S. (1992) *Proc. Nat. Acad. Sci. U. S. A.* **89,** 3541–3545
36. Demaurex, N., Grinstein S., Jaconi M. E., Schlegel W., Lew D. P., and Krause K. H. (1993) *J. Physiol.* **466,** 329–344
37. Lukacs, G. L., Kapus, A., Nanda, A., Romanek, R. R., and Grinstein, S. (1993) *Am. J. Physiol.* **265,** C3–C14